Institute of Space and Aeronautical Science, University of Tokyo
Report No. 486, July, 1972

Free Jet Expansion from Concentric Orifices into Vacuum

By

Hakuro OGUCHI, Shun-itsu SATO and Osamu INOUE

Summary: In a separate issue of two different molecular-weight gases through the concentric orifices into a vacuum, both density measurement and flow visualization are made by means of the electron beam fluorescence technique. In the experiment, the nitrogen is used as heavier gas and the helium as lighter gas. The gasdynamical interaction between outer jet of heavier (or lighter) gas and inner jet of lighter (or heavier) gas is examined, and specifically the density behavior of the gas species issued from inner orifice is clarified.

1. INTRODUCTION

The specification of a free jet issuing into a vacuum is primarily needed for the production of a high energy molecular beam in laboratories. Recently this is also urgently required for knowledge of the flow field of the rocket exhaust at an upper high-altitude atmosphere. With a recent development of experimental techniques, say a successful application of electron beam fluorescence technique, many experimental works have been done on free jet problems of both single component gases and gases mixture [*1*]–[*6*]. As regards analytical works, Sherman [*7*] analysed a source flow expansion into a vacuum from continuum aspect, and suggested that the flow along axis of a free jet into a vacuum may be closely simulated by a source flow expansion. Following his work, the various theoretical approaches to the problem have been motivated based upon molecular aspect [*8*]–[*13*]. The source expansion flow as well as free jet into a vacuum are basically important phenomena from either a physical or an engineering point of view. An analytical treatment of a source flow is much easier than that of a free jet, while its achievement in laboratories is likely to be more difficult task. In the previous report [*14*], the structure of inner core in the free jet into a vacuum was investigated with special regard to a simulated nature to the source expansion flow by using the same experimental apparatus as in the present experiment.

In the present paper we also consider a separate issue of the different molecular-weight gases into a vacuum through concentric orifices from the respective plenum vessels (Fig. 1). The aim of the present experiment is to clarify the characteristic features pertinent to such a separate issue of two different gases into

a vacuum, and also to examine the gasdynamical interaction between outer jet of heavier (or lighter) gas and inner jet of lighter (or heavier) gas. Specifically our main concerns are with the problem of the confinement of the inner gases species by the outer jet.

2. Experimental Apparatus

In Fig. 1 is shown a schematic diagram of the experimental apparatus. The apparatus consists of (1) coaxial nozzle with concentric orifices, mounted on a drive unit, (2) an electron gun system for generating the electron beam, (3) an optical system measuring the luminosity of the light emitted from concerned segment of the electron beam, (4) a flow visualization system with a camera mounted on another drive unit, and (5) vacuum system.

The coaxial nozzle was made of brass, consisting of an inner orifice (2 mm in diam.) and an outer one (9 mm in diam.). These are connected through 10 mm in diam. tubes separately to a pair of vessels placed outside the test chamber. Both test chamber (50 cm diam., 60 cm long) and electron gun chamber (10 cm diam., 12 cm high) were evacuated by separate vacuum systems. Both sides of the test chamber have a pair of 10 cm diam. windows for the optical detection and flow visualization. The lowest pressure attainable in the test section was about 10^{-3} Torr by a combination of 5 HP rotary, mechanical booster and 10 in. oil diffsion pumps. The test gases (commercially pure nitrogen and helium) were discharged into the test chamber through inner and outer orifices from the separate vessels. The capacity of the vacuum system was not sufficient for continuous issue to maintain the test chamber pressure lower as desired, and thus the issue of gases was only allowed for a short period, say about 0.5 sec.

The electron beam system consists of an electron gun capable of producing a narrow, high energy electron beam and a collector cup for detection of the electron

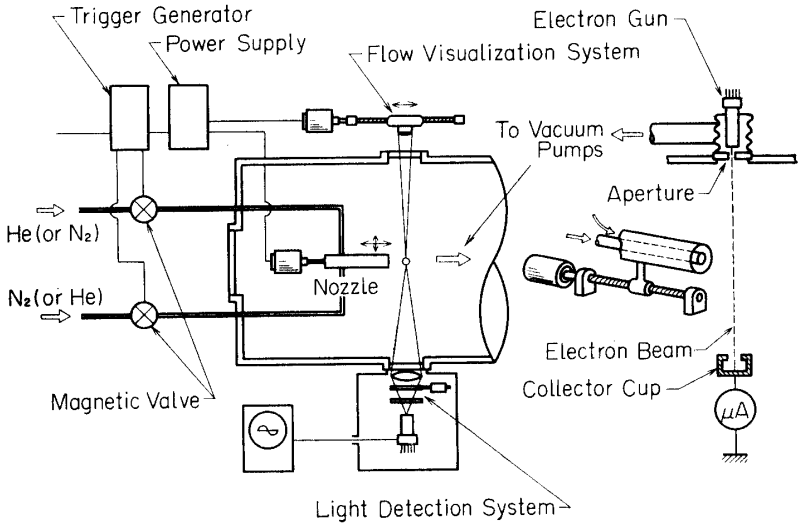

Fig. 1. Schematic diagram of apparatus.

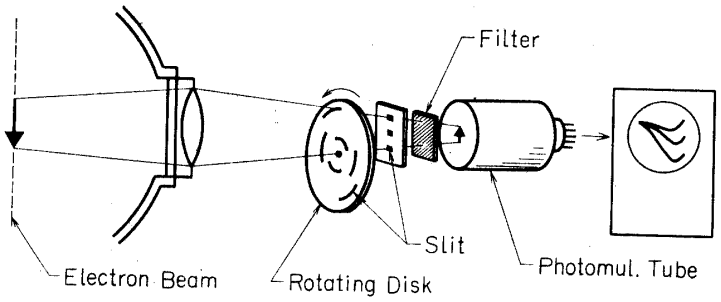

FIG. 2. Optical detection system.

beam current. The electron gun was placed in a vacuum chamber, in which the pressure could be maintained below 1×10^{-4} Torr throughout experiments. The acceleration potential was 16 KV and the beam current 200 μA. Two sets of the electrostatic deflector were also equipped in the gun for adjustment of the beam direction. The elctron gun was mountd on the test chamber through the bellows joint for a mechanical adjustment of the beam direction. The electron gun was of the type similar to a commercial TV tube, but a tungsten filament was used instead of the oxide-coating cathode.

A schematic view of the light detection system is shown in Fig. 2. The image of the light beam, which was produced by electron beam impact, was forcused through a lens on a rotating disk with several circular slits, through which the light can pass alternately. In the experiment the disk was rotated by motor at about 6,000 r.p.m. Just behind the disk were installed an interference filter and a photomultiplier tube, the output signal of which was recorded on an oscilloscope. This optical detection system makes possible to obtain a simultaneous record of luminosity of the light emitted from several segments on the beam. Actually this was done only for measurement of the density pattern on the meridian plane, on which the jet axis lies. As regards the density pattern over a cross section normal to the jet axis, however such a simultaneous record was not necessary, because the flow phenomena concerned are axially symmetric.

3. EXPERIMENTAL CONDITIONS

The experiment was made on the following cases, (1) issuing nitrogen from the outer orifice and helium from the inner orifice, and (2) issuing helium from the outer orifice and nitrogen from the inner orifice. For convenience, we designate these as Case I and Case II, respectively. In this experiment we use nitrogen as heavier gas, and helium as lighter gas. Various stagnation pressures P_i of the inner jet were chosen for a fixed one P_o of the outer jet, say 100 Torr.

In application of the electron beam fluorescence method, the light intensity emitted from the gases species concerned is related to the species number density by an appropriate choice of the wave length. An appropriate choice of the wave length for various gases is suggested based on comprehensive data (for example,

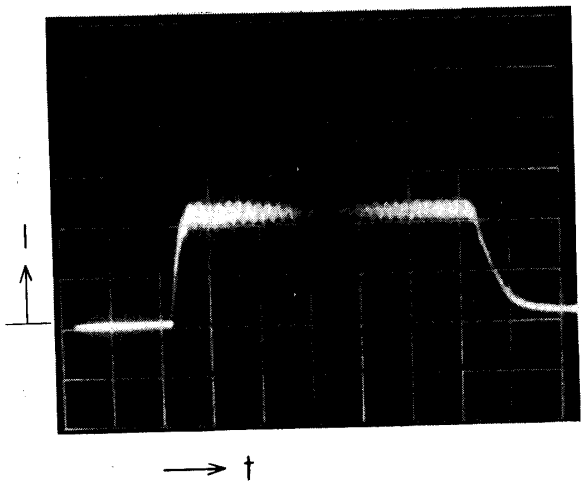

FIG. 3. Time history of luminosity at a point fixed relatively to the nozzle (100 m sec/div.).

see [15]–[17]). Following the references, we chose a line of 5,016 Å for helium and the head (4,278 Å) of 0–1 band in spectrum of nitrogen. The relation of the species number density to the light intensity was able to be determined by a method of static calibration with the same optical system as employed in the density measurement. Such a calibration was made up to a comparatively higher density by using a fast acting valve equipped just outside of the electron gun apertuer (2 mm diam. and 20 mm long). Otherwise, the filament of electron gun might have seriously been damaged by an anomalous pressure rise in electron gun.

Since the issue of gases is made only during a short period, the establishment of the stationary flow must primarily be checked. The light intensity from a fixed point on the jet axis was measured without driving nozzle. An oscilloscope record is shown in Fig. 3. As can be seen from this record, the flow was found to be nearly stationary over a wide intermediate region except the short periods around both start and stop of the flow.

4. Density Distribution Along the Jet Axis

The density distribution along the jet axis was determined from the data obtained by the measurement by means of the electron fluorescence technique mentioned before, in which case the nozzle was moved along the jet axis toward the downstream normal to the electron beam fixed. One of the typical oscilloscope records is shown in Fig. 4. The time scale t can simply be deduced to the distance x, measured from the nozzle exit to the downstream along the jet axis, by multiplication of the driving speed of nozzle.

The analyses for a source or spherical expansion flow into a vacuum have already been worked out by several authors from both continuum [7], [18] and kinetic aspects [8]–[13]. If the flow is entirely in thermal equilibrium, the flow

quantities can properly be represented by the isentropic theory. It was confirmed by the existing analyses that, even if the flow is thermally non-equilibrium due to rarefaction effects, the density behavior is very close to that predicted by the isentropic theory. If our concern is restricted to a region downstream far from the source, the density is simply related to the coordinate x, as

$$\rho/\rho^* = (x/x^*)^{-2},$$

where the asterisks refer to the sonic condition.

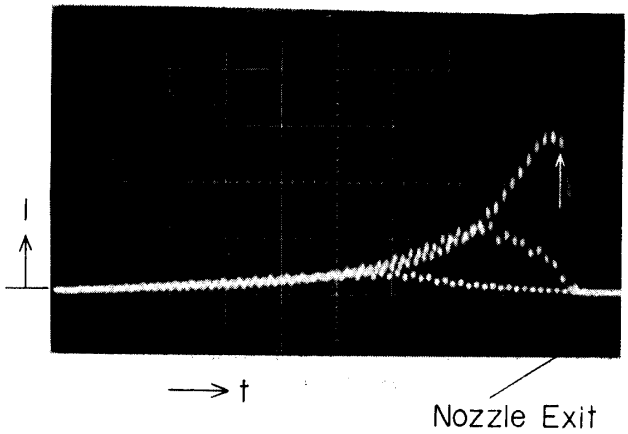

FIG. 4. Simultaneous record of luminosity along the lines parallel to the jet axis (50 m sec/div.).

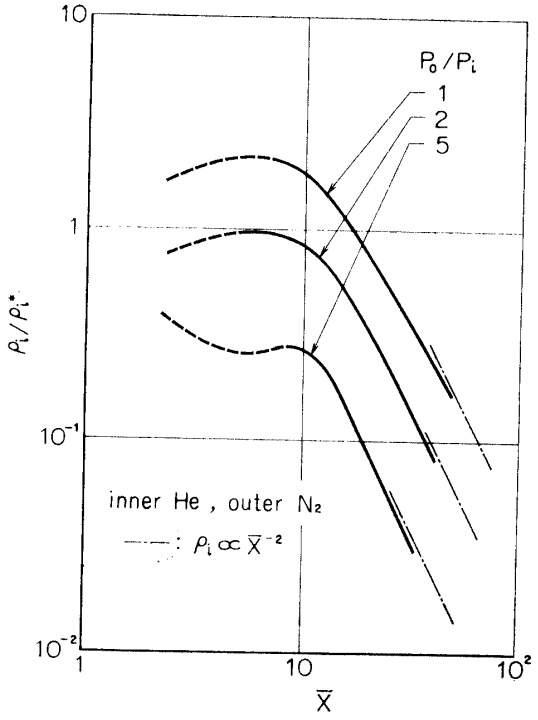

FIG. 5. Density distribution along the jet axis for Case I.

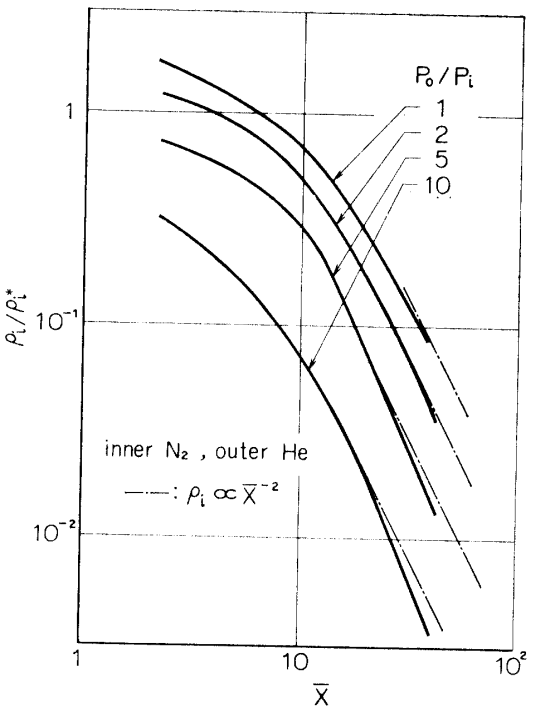

FIG. 6. Density distribution along the jet axis for Case II.

Bearing in mind the above fact, we plotted the inner gas species density ρ_i against $\bar{x}$ ($=x/d$, d: inner orifice diameter). These plots are shown in Figs. 5 and 6, respectively, for Cases I and II. It can be seen from these figures that in a region far from the exit the density decreases nearly in proportion to the inverse square of the distance x, as was predicted by the analyses for a source flow. The similar nature was found for the density behavior along the jet axis in expansion from a single nozzle into a vacuum [6].

5. Density Distribution Over the Cross Section at Various Axial Locations

The density distribution along the radial line on the cross section at a given axial location was determined from the data obtained by means of the electron beam fluorescence technique, in which case the nozzle was moved in the direction normal to both jet axis and electron beam. One of the typical oscilloscope records is shown in Fig. 7. The density distributions, which was derived from the records taken for several axial locations, are shown in Figs. 8 and 9, respectively, for Case I and for Case II with the stagnation pressure ratio $P_o/P_i=1.0$ ($P_o=P_i=100$ Torr), and in Figs. 10 and 11, respectively, for Case I and for Case II with the stagnation pressure ratio $P_o/P_i=2.0$ ($P_o=100$ Torr, $P_i=50$ Torr). The dimensionless coodinates ($\bar{x}$, $\bar{r}$) are referred to the diameter d of inner orifice, i.e. $\bar{r}=r/d$, $\bar{x}=x/d$. The dimensionless density $\bar{\rho}$ is defined by ρ/ρ_o with ρ_o, the density of gases species at the normal temperature and pressure.

With the exceptional interests in behavior of the inner gas species, the density profile $\bar{\rho}_i$ ($\bar{r}$) of the gas issued from the inner orifice was found to be well fitted to the Gaussian profile

$$\bar{\rho}_i(\bar{r})=\bar{\rho}_{i0}\exp(-\lambda\bar{r}^2), \tag{1}$$

where $\bar{\rho}_{i0}$ is the dimensionless density on the axis $r=0$. The magnitude of λ provides a measure for spread of the inner gas species. Apparently both $\bar{\rho}_{i0}$ and λ depend on x. In Fig. 12 the λ derived from the data is plotted against $\bar{x}$, with those obtained for the case of the single jet issued from inner orifice alone. This figure shows that the gas species from the inner orifice is confined by that from the outer orifice, and that the spread of the inner gas species strongly depends on the molecular weight ratio to the outer gas species. In fact, as can be seen from Fig. 12, more remarkable confinement of the inner gas species is achieved in Case I than in Case II.

The mass conservation of the gas species issuing from the inner orifice yields

$$I=2\pi\int_0^\infty \bar{\rho}_i U_i \bar{r}\,d\bar{r}=2\pi\bar{U}_i\int_0^\infty \bar{\rho}_i\bar{r}\,d\bar{r}=\text{const.}, \tag{2}$$

where U is the axial velocity, $\bar{U}$ the mean axial velocity, and the subscript "i" refers to the quantities pertinent to the gas species issued from the inner orifice. The integral I in Eq. (2) was evaluated from data for the various axial locations,

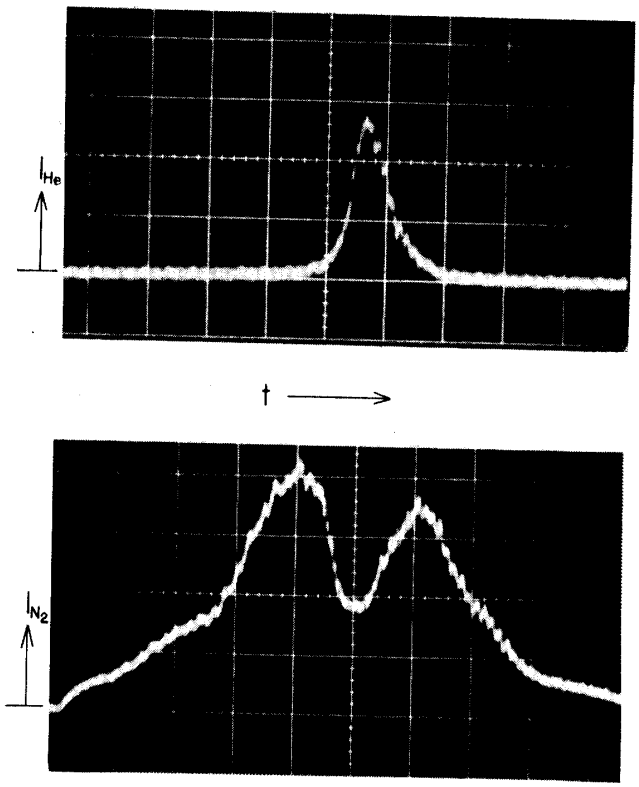

FIG. 7a. Luminosity of the gases species in a cross section normal to the jet axis for Case I (50 m sec/div.).

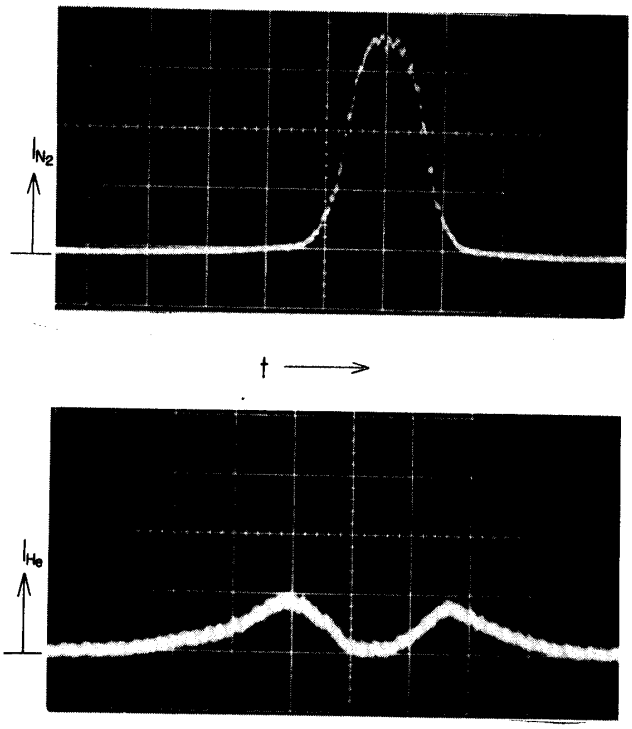

FIG. 7b. Luminosity of the gases species in a cross section normal to the jet axis for Case II (50 m sec/div.).

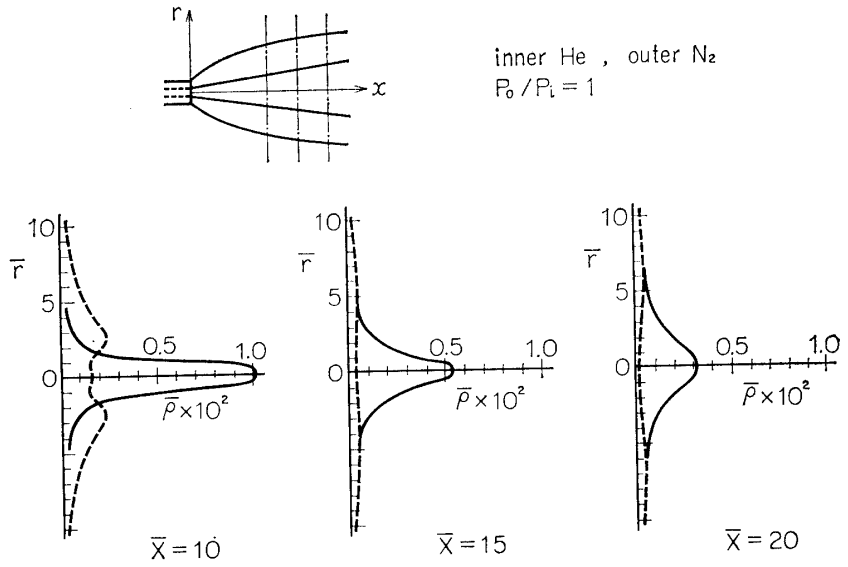

FIG. 8. Density distributions of the gases species in various cross section normal to the jet axis for Case I with $P_o/P_i=1$.

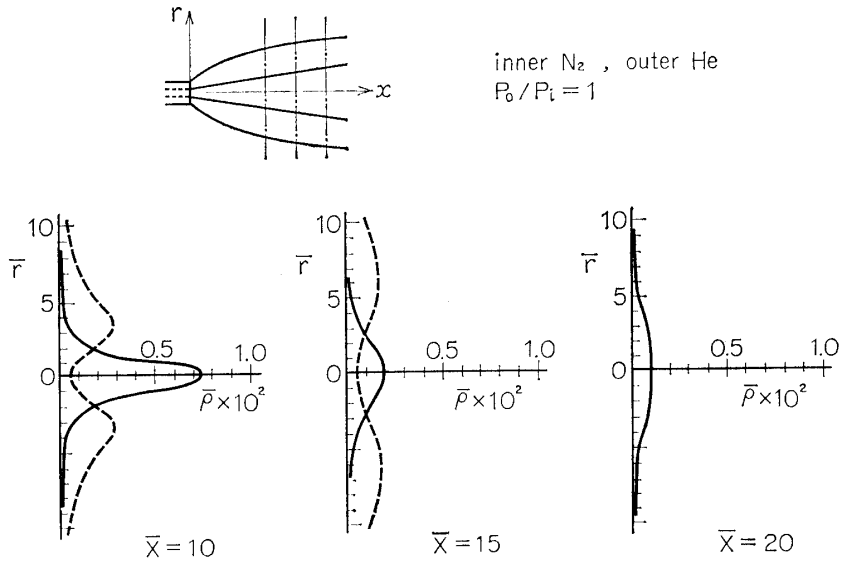

FIG. 9. Density distribution of the gases species in various cross sections normal to the jet axis for Case II with $P_o/P_i=1$.

TABLE 1. Ratio of the Density Integral J $(=I/2\pi\bar{U}_i)$.

Case	$\frac{P_o}{P_i}$	$\frac{J(\bar{x}=15)}{J(\bar{x}=10)}$	$\frac{J(\bar{x}=20)}{J(\bar{x}=15)}$
I	1	0.97	—
I	2	0.94	—
II	1	0.88	0.95
II	2	0.78	0.88

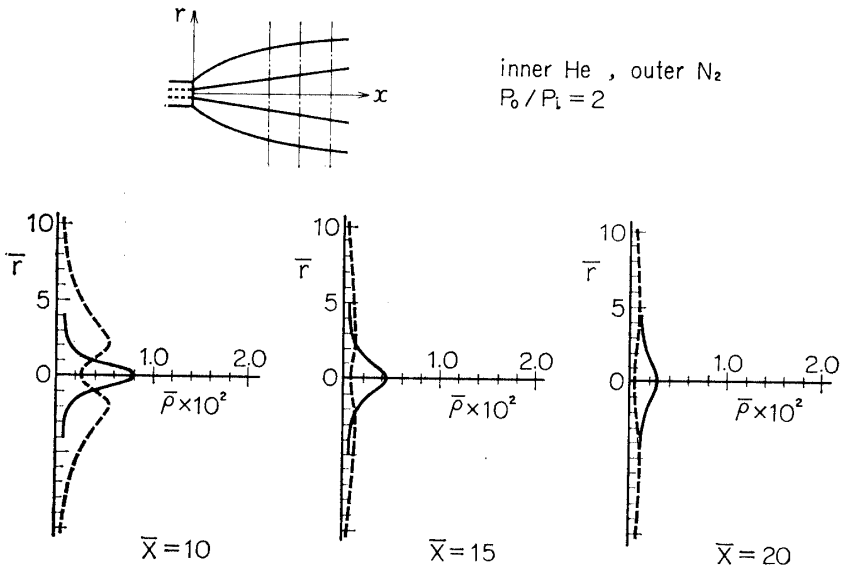

FIG. 10. Density distribution of the gases species in various cross sections normal to the jet axis for Case I with $P_o/P_i=2$.

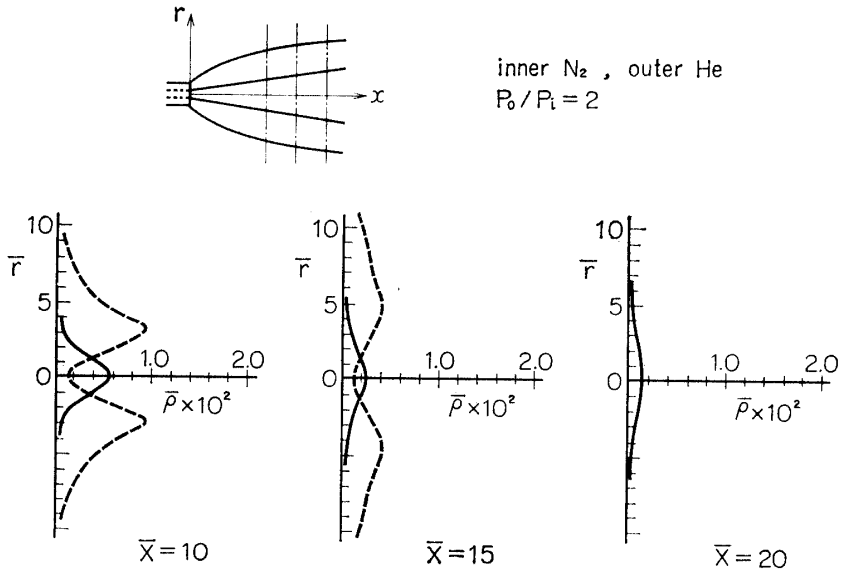

FIG. 11. Density distribution of the gases species in various cross sections normal to the jet axis for Case II with $P_o/P_i=2$.

say $\bar{x}=10$, 15 and 20. The ratios of integral I between different axial locations are listed in Table 1. As can be seen from this table, the density integral I is so weakly dependent on the axial location. From the conservation relation, U_i is nearly independent of $\bar{x}$, so that it may be very close to the terminal velocity over the region concerned.

If, as shown above, the density profile of the gas species from inner orifice is represented by the Gaussian, Eq. (2) gives

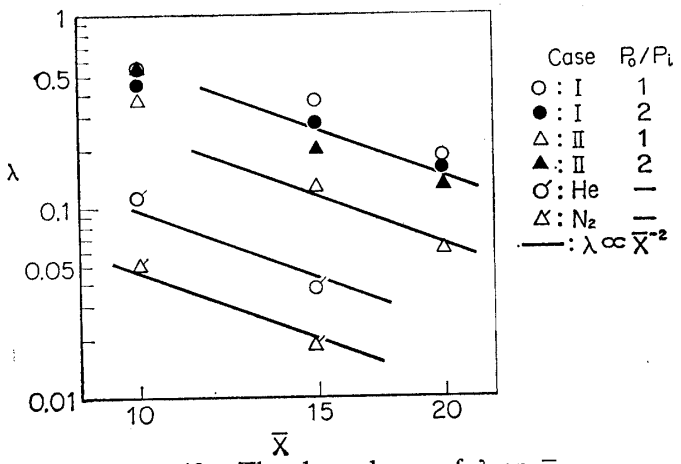

FIG. 12. The dependence of λ on $\bar{x}$.

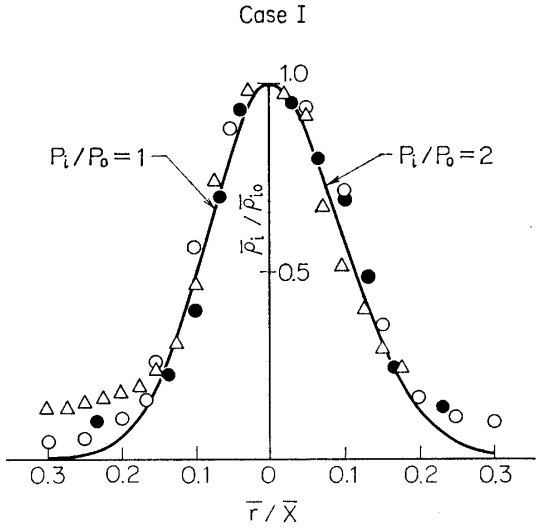

FIG. 13. Cross-sectional density profile of the inner gases species (Case I) (○; $\bar{x}=10$, ●; $\bar{x}=15$, △; $\bar{x}=20$).

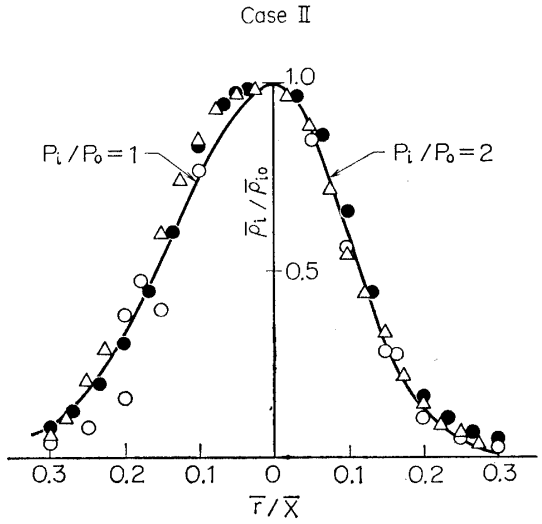

FIG. 14. Cross-sectional density profile of the inner species (Case II) (○; $\bar{x}=10$, ●; $\bar{x}=15$, △; $\bar{x}=20$).

$$\bar{U}_i\bar{\rho}_{i0}/\lambda=\text{const.}$$

Suppose that $\bar{U}_i$ may be regarded as a constant independent of $\bar{x}$. Since, as shown in the previous section, the density $\bar{\rho}$ along the jet axis is nearly proportional to $\bar{x}^{-2}$, we obtain from the above relation

$$\lambda\propto\bar{x}^{-2} \tag{3}$$

In Fig. 12 this relation is referred in comparison with the experimental data. We can see that the relation of Eq. (3) reasonably fits the data with a few exceptions.

Summarizing the foregoing argument, we say that in a separate issue of different gases from the concentric orifices into a vacuum, the density profile of gas species from inner orifice may properly be expressed by the Gaussian profile

$$\bar{\rho}_i=\bar{\rho}_{i0}\exp\left[-\lambda_0(\bar{r}/\bar{x})^2\right] \tag{4}$$

For comparison with this, the experimental data are re-plotted in Figs. 13 and 14. It should be noted that, for an orifice geometry fixed, the factor λ_0 is dependent on both molecular weight and stagnation pressure ratios between inner and outer gases species.

6. Flow Visualization

In what follows the flow visualization method and the results will be described. For an electron beam fixed, the nozzle is moved along the jet axis in the direction downstream normal to the beam. If one moves with the nozzle, then one can view a flow pattern scanned by an electron beam during the testing time. Therefore one can take a picture of the flow pattern by moving a camera at a speed fixed relatively to the nozzle. In that case the camera shutter must be synchronized so as to open just during the time period between start and stop of the flow. Figures* 15 and 16 are the pictures thus taken, respectively, for Case I and for Case II with the stagnation pressure ratio $P_o/P_i=1.0$. The light emitted from nitrogen has a spectrum different from that of helium. Therefore, in the pictures the distributions of both nitrogen and helium gases species are distinguishable from each other.

The pictures shown above provide a qualitative but intuitive view on the flow pattern concerned. The flow is rather complicated in the vicinity of the flow exit, so that the mixing between inner and outer gases species could not be avoided at the initial stage of expansion. As can be seen, the outer gas species interfusing into the inner core of jet appears to be mainly due to this mixing at the initial stage of expansion. In a moderately downstream region of concern, however the

* All the pictures shown here were taken for the stagnation pressures ($P_o=P_i=400$ Torr) higher than those in the density measurements, because otherwise the luminosity of gases species was not sufficient to view a detail flow pattern. The films used were Kodak high-speed ektachrome (color) and Trix-X pan film, respectively, for Figs. 15a and 16a, and for Figs. 15b and 16b.

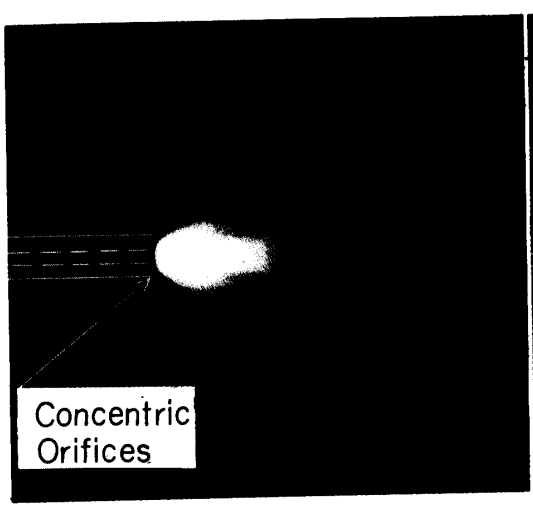

FIG. 15a. Flow visualization for Case I.

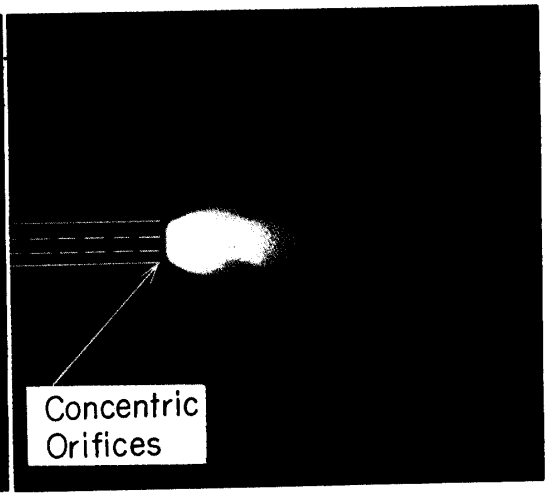

FIG. 16a. Flow visualization for Case II.

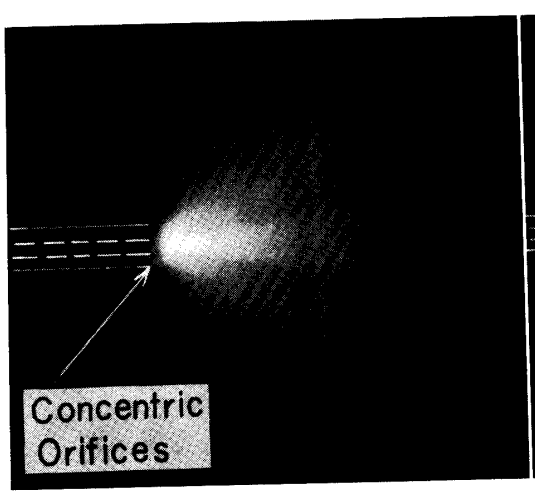

FIG. 15b. Flow visualization for Case I.

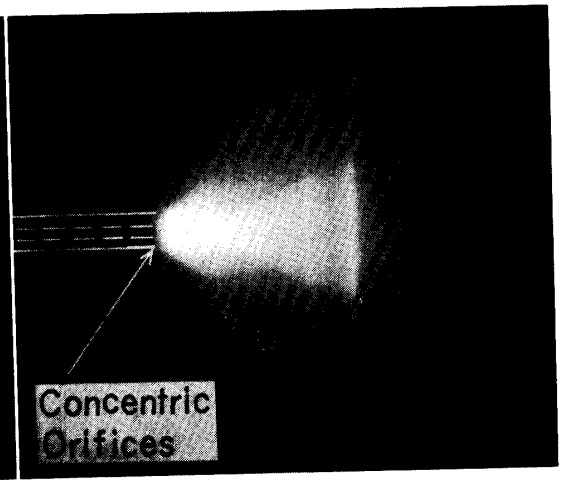

FIG. 16b. Flow visualization for Case II.

mixing occurs much less than in the vicinity of exit, and both outer and inner gases species indicate an appreciably distinct separation from each other. The characteric features of flow, which were observed by the flow visualization, are in reasonable agreement with the results of the density measurements.

7. Concluding Remarks

In a separate issue of different molecular-weight gases from the concentric orifices into a vacuum, both density measurements and flow visualizations were made by means of the electron beam fluorescence technique.

As regards the density distribution along the jet axis, that of the gas species issued from the inner orifice is found to be represented by a source or spherical expansion-like nature, so far as a moderate downstream is concerned. The measurement of the density distribution in a cross section normal to the jet axis shows that the gas species issued from the inner orifice is well confined by that from

the outer orifice, and that its cross-sectional density profile can properly be fitted to the Gaussian profile. From both density measurements and flow visualizations it is found that the inner gas species is much sharply confined by issue of heavier gas from the outer orifice than done by issue of the lighter gas, and that at a moderate downstream the mutual interfusion between inner and outer gases species is much less than that at the initial stage of expansion.

Finally we note that the flow characteristics of the separate issue of different molecular-weight gases from the concentric orifices into a vacuum are subject to the following parameters; the molecular-weight ratio of gases species, the stagnation pressure ratio and the orifices geometry, but the effect of variation in the last parameter was not examined. To clarify more general features relevant to the phenomena concerned, further study will be required from both sides of experiment and analysis.

8. Acknowledgements

The authors would like to express sincere thanks to Messrs. H. Minami and H. Tsuruzoe of Tokyo Shibaura Electric Co., Ltd. for their kind cooperation in design and preparation of the electron gun used in the present experiment.

Department of Aerodynamics
Institute of Space and Aeronautical Science
University of Tokyo, Tokyo
July 10, 1972

References

[1] P. C. Waterman and S. A. Stern, *J. Chem. Phys.*, **31**, 405 (1959).
[2] H. Mikami and Y. Takashima, *Bull. Tokyo Inst. Tech.*, **61**, 67 (1964).
[3] D. E. Rothe, *Phys. Fluids*, **9**, 1643 (1966).
[4] H. Ashkenas and F. S. Sherman, in *"Rarefied Gas Dynamics"*, (ed. J. H. de Leeuw), Academic Press, New York, Vol. II, 84 (1966).
[5] D. I. Sebacher, *AIAA J.*, **6**, 51 (1968).
[6] A. E. Beylich, *Phys. Fluids*, **14**, 898 (1971).
[7] F. S. Sherman, *Phys. Fluids*, **8**, 773 (1965).
[8] J. W. Brook and R. A. Oman, in *"Rarefied Gas Dynamics"*, (ed. J. H. de Leeuw), Academic Press, New York, Vol. I, 125 (1965).
[9] R. H. Edwards and H. K. Cheng, *AIAA J.*, **4**, 558 (1966).
[10] B. B. Hamel and D. R. Willis, *Phys. Fluids*, **9**, 829 (1966).
[11] T. Soga, ISAS Report No. 478, Institute of Space and Aero. Sci., University of Tokyo, Vol. 37 (1972).
[12] G. A. Bird, *AIAA J.*, **8**, 1998 (1970).
[13] T. Soga and H. Oguchi, *Phys. Fluids*, **15**, 766 (1972).
[14] H. Oguchi, S. Sato and O. Inoue, *Trans. Japan Soc. of Aero. Sci.*, **14**, 72 (1971).
[15] B. W. Shumacher and E. O. Gadamer, *Canadian J. Phys.*, **36**, 659 (1962).
[16] E. P. Muntz, *Phys. Fluids*, **5**, 80 (1962).
[17] E. W. Becker, K. Bier and W. Henkes, *Z. Physik*, **146**, 333 (1965).
[18] P. L. Owen and C. K. Thornhill, Aeronautical Research Council, R. & M., 2616 (1948).